



Sedimentary and diagenetic environments of Middle Ordovician iron-rich limestones (Pobroszyn Formation) in the northern Holy Cross Mountains, Poland

Wiesław TRELA



Trela W. (2008) — Sedimentary and diagenetic environments of Middle Ordovician iron-rich limestones (Pobroszyn Formation) in the northern Holy Cross Mountains, Poland. *Geol. Quart.*, 52 (3): 199–212. Warszawa.

The Middle Ordovician (Dapingian) of the northern Holy Cross Mountains (central Poland) is represented by condensed limestones that make up the Pobroszyn Formation. They reveal a complex stratification reflecting alternating depositional conditions. The basal limestones were deposited in open-marine conditions during the early Middle Ordovician sea level rise (*navis* Zone) correlated with the Baltoscandian Gårdlosa drowning. Periods of non-deposition associated with this transgression favoured precipitation of authigenic Fe minerals close to the sediment-water interface. The upper part of this succession appears to represent a succeeding depositional phase associated with a second transgressive event, which probably involved reworking of the underlying lithified substrate. High energy events were interrupted by periods of non-deposition favouring development of benthic microbial communities contributing to Fe authigenesis. The Pobroszyn Formation reveals features suggesting an early diagenetic alteration of the parent carbonate sediment in a shallow marine setting (e.g., beach shoreface) or even was influenced by meteoric diagenesis, which probably took place during a sea level fall preceding the second transgressive event.

Wiesław Trela, Polish Geological Institute, Holy Cross Mts. Branch, Zgoda 21, PL-25-953 Kielce, Poland; e-mail: wieslaw.trela@pgi.gov.pl (received: June 24, 2008; accepted: July 22, 2008).

Key words: Ordovician, limestones, ironstones, reworking, diagenesis.

INTRODUCTION

This paper discusses sedimentary and diagenetic environments of Middle Ordovician limestones in the northern Holy Cross Mountains (HCM, central Poland) in the context of sea level changes. The northern HCM is an exposed segment of the Łysogóry Unit, which to the south contacts with the Małopolska Massif along the Holy Cross Fault (Fig. 1). In the Middle Ordovician both of these terranes were located in the marginal region of Baltica (Dadlez *et al.*, 1994; Cocks and Torsvik, 2005; Nawrocki *et al.*, 2007) within a temperate/cool water realm of the southern high latitude belt (Trela, 2005, 2008). Thus, the sea level history reconstructed for Baltoscandia (Nielsen, 2004) appears to be a good background for processes discussed in this paper.

Several lines of evidence suggest that the Middle Ordovician limestones from the northern HCM were subjected to diagenetic alteration dependent on the mineralogical composition of the parent carbonate sediment, that accumulated within a cool/temperate water environment. However, some

features suggest an influence of meteoric waters upon the microfabric pattern of the limestone. Meteoric diagenesis and pedogenic horizons are used as evidence of subaerial exposure in marine carbonate successions (Read and Grover, 1977; Esteban and Klappa, 1983; Choquette and James, 1988; Tucker and Wright, 1990; Wright, 1994; Moore, 2001). However, in the case of the Ordovician, the recognition of meteoric overprinting and pedogenic processes is hampered by a lack of diagnostic features produced by plants. Van Houten (1985) suggested that the higher CO₂ level of the Ordovician atmosphere contributed to more acidic groundwaters at high latitude, which resulted in weathering similar to that observed today in forested tropical settings.

The Ordovician succession in the northern HCM was studied in the context of the stratigraphic and tectonic evolution of this region (Dzik, 1999; Trela *et al.*, 2001; Trela, 2006a and references herein). A preliminary interpretation of the sedimentary environment of the limestone studied has been proposed by Trela *et al.* (2001) and Trela (2003). However, none of these studies have discussed details of marine authigenesis and diagenesis, and their relation to sea level fluctuation.

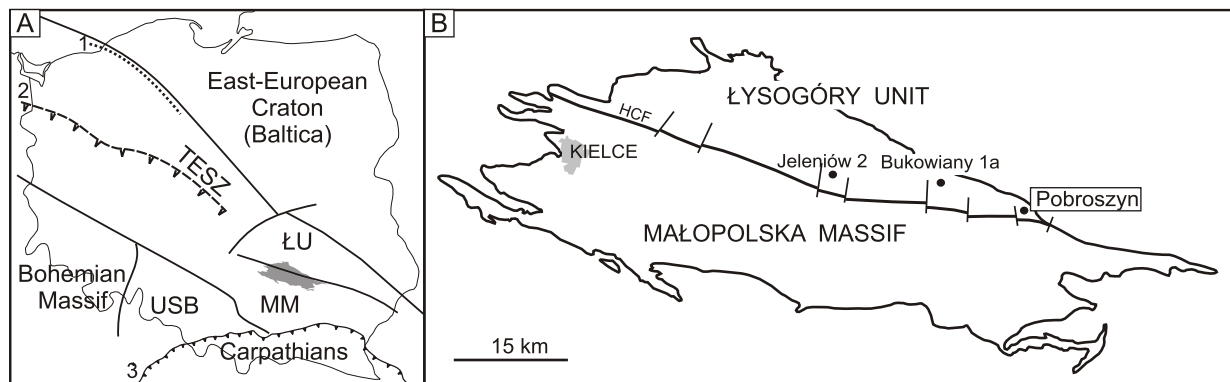
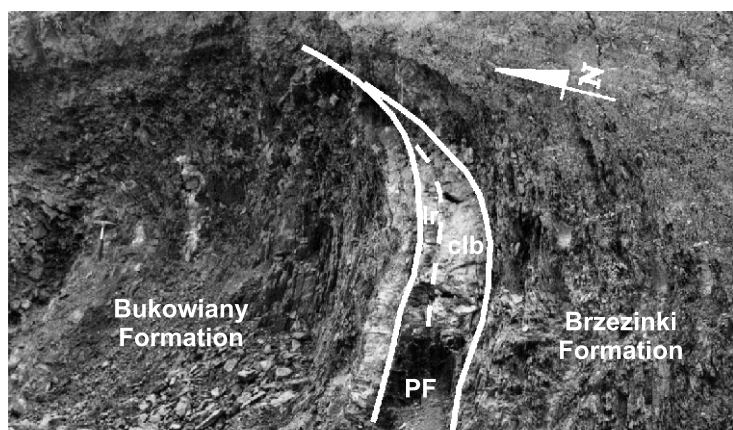


Fig. 1. Location of the Holy Cross Mountains (A) and the Pobroszyn section (B)

ŁU — Łysogóry Unit; MM — Małopolska Massif; USB — Upper Silesian Block; 1 — Caledonian front; 2 — Variscan front; 3 — Alpine front; HCF — Holy Cross Fault; TESZ — Trans-European Suture Zone



MATERIAL AND METHODS

Detailed sedimentological studies were carried out on limestones of the Pobroszyn Formation, which are exposed at Pobroszyn, in the eastern part of the northern HCM (Figs. 1 and 2). The lithological and sedimentological observations of this limestone included: rock colour, lithology, sedimentary structures and stratification types. Petrographic description is based on study of more than 30 stained and unstained thin sections. These studies were supplemented by electron microprobe analyses using a *Leo 1430* scanning microscope equipped with an *EDS-ISIS 300* system. Small pieces of selected samples were observed under a scanning electron microscope (SEM) after slight etching with diluted HCl to enhance micromorphology. Thin sections were polished and examined under cathodoluminescence (CL) microscopy to determine cement growth patterns. CL analysing was performed using a *Nicon Optiphot 2* polar microscope linked with a Cambridge Image Technology Ltd. cathodoluminescence unit CCL 8200 mk3. General operating conditions for CL were a beam voltage of 12 to 15 kV and a beam current of approximately 0.6 mA.

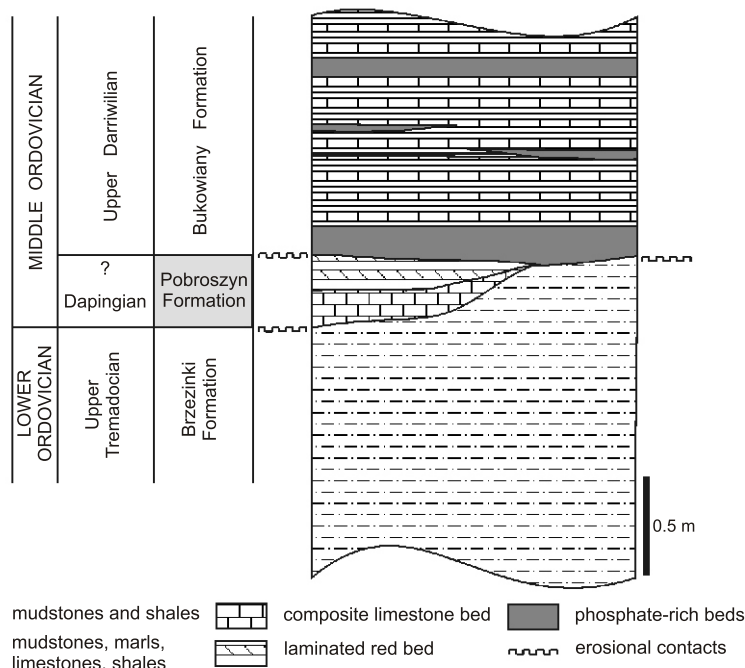


Fig. 2. Lithological and stratigraphical section of the Ordovician succession in Pobroszyn (stratigraphy after Trela *et al.*, 2001; Trela, 2006a)

GEOLOGICAL BACKGROUND AND STRATIGRAPHY

In the type locality (Pobroszyn), the base of the Pobroszyn Formation is defined by a conspicuous discontinuity (Fig. 2), which separates the limestones studied from the

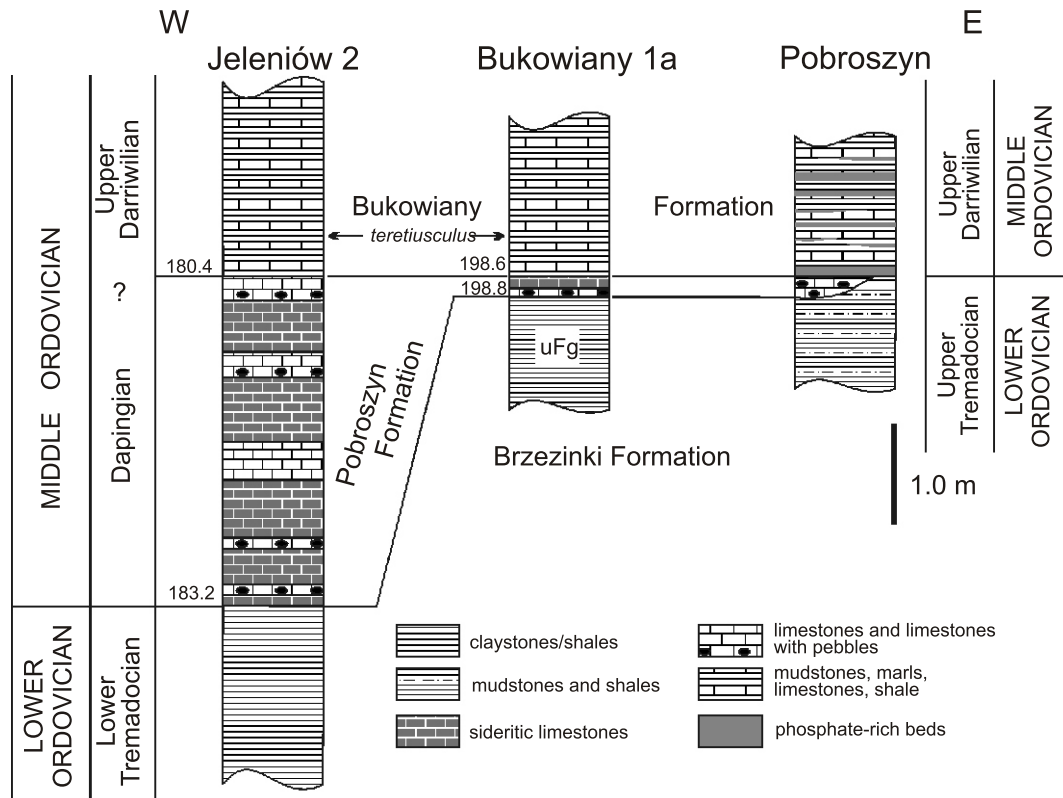


Fig. 3. Correlation of the Middle Ordovician limestone between the Pobroszyn section and the Jeleniów 2 and Bukowiany 1a boreholes (stratigraphy after: Tomczyk and Turnau-Morawska, 1967; Trela *et al.*, 2001; Trela, 2006a)

uFg — upper Furongian

underlying mudstones and shales of the Brzezinki Formation, dated by acritarchs diagnostic for the uppermost Tremadocian (Trela *et al.*, 2001; Trela, 2006a). Conodont data indicate that the Pobroszyn Formation lies within the *Baltoniodus navis* Zone (Dzik, 1999) and therefore can be correlated with the Dapingian global stage of the Middle Ordovician. The overlying phosphate-rich succession belongs to the Bukowiany Formation and correlates with the upper Darrivilian and Sandbian global stages (Trela, 2006a, 2008). The contact with the Bukowiany Formation is also marked by a conspicuous discontinuity with a hiatus corresponding to the lower or even middle part of the Darrivilian stage (Trela, 2006a, 2008; Fig. 2).

The thickness of the Pobroszyn Formation increases westwards, to 2.8 m in the Jeleniów 2 borehole (Fig. 3) where it rests upon the lowermost Tremadocian claystones of the Brzezinki Formation (Trela, 2006a). However, in the Bukowiany 1a borehole a hiatus between the Pobroszyn and Brzezinki formations includes also the lowermost Tremadocian (Fig. 3). The bulk of the Pobroszyn Formation in both of the boreholes studied is made up of greenish sideritic limestones intercalated with finely crystalline limestones containing dispersed or concentrated pebbles and intraclasts of variable lithology (up to 3 cm long), quartz grains and skeletal fragments (Tomczyk and Turnau-Morawska, 1967). The sideritic limestones reveal colour mottling and contain green ooids

and pisoids (up to 1 cm in diameter) with a well-preserved laminar structure cut by septarian-like micro-cracks (Tomczyk and Turnau-Morawska, 1967). The pebbles are mostly composed of dark cherty shales and phosphorites, whereas intraclasts consist of carbonate rocks.

In the southern HCM, the Pobroszyn Formation correlates with variegated mudstones and carbonates of the Szumsko Formation overlain by bioturbated sandstones with coquina interbeds of the Bukówka Formation (Trela, 2006a), which form a narrow belt passing southwards into grey/green shales of the Brzeziny Formation (Fig. 4).

SEDIMENTARY AND PETROGRAPHIC DESCRIPTION

The Pobroszyn Formation in the section studied is represented by two beds, each revealing different stratification. They are referred to as the basal composite limestone bed (up to 25 cm thick — clb) and the overlying laminated red bed (lr), up to 15 cm thick (Figs. 5 and 6). The composite limestone bed is well dated by conodonts of the *Baltoniodus navis* Zone (Dzik, 1999). Unfortunately, until now, the laminated red bed lacks any biostratigraphic data that might allow its precise stratigraphic correlation.

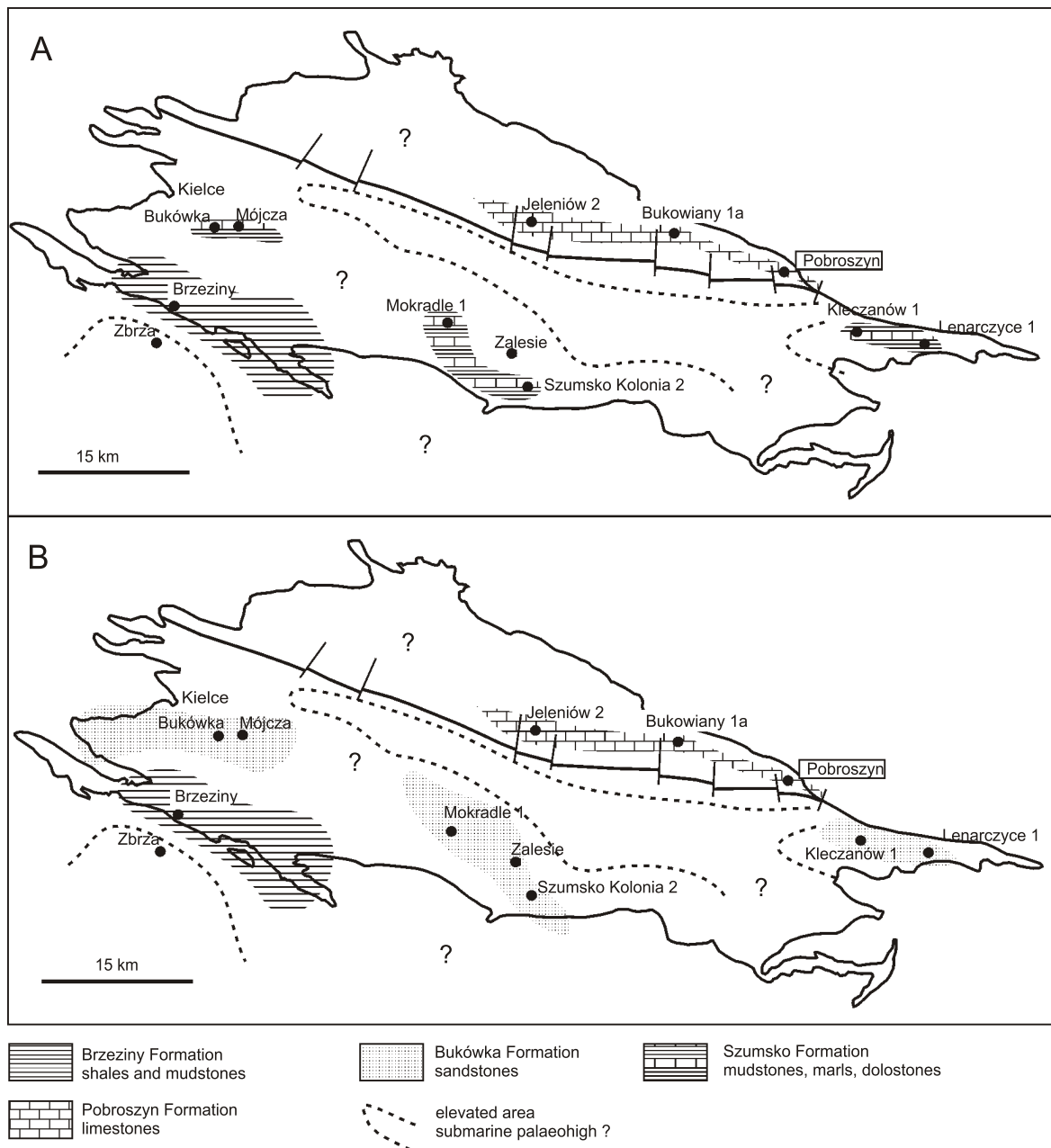


Fig. 4. Distribution of the Middle Ordovician lithostratigraphic units in the Holy Cross Mts.

A — Dapingian (*navis* conodont zone), B — lower and middle Darriwilian

COMPOSITE LIMESTONE BED (CLB)

This bed displays a composite internal stratification pattern, and thus can be divided into two levels (Fig. 5A). However, laterally one of these levels can be missing resulting in significant reduction of the bed's thickness.

Level I — reveals characteristic red colour mottling on a grey/green background (Fig. 5). The incipient sediment brecciation and red hematite staining (blisters, holes, microtufts, perforation and microfissure infillings) are common features of this level (Fig. 5A). Thin calcite layers (up to 3 cm thick) and lenses occur at the base of this unit (Fig. 5B, C). Moreover, this level contains phosphorite pebbles (up to 3 cm long) and mono- to polycrystalline quartz grains (up to 1 cm in

diameter) scattered within the carbonate groundmass (Fig. 5A, C). These are accompanied by black coated grains, up to 1–4 mm in diameter, “floating” together with the dark clotted sediment in the host limestone (Figs. 5C and 7). In places, small-scale and Fe-impregnated discontinuity surfaces, encrusted by tiny Fe stromatolites and accompanied by small iron superficial ooids (up to 0.7 mm in diameter), occur within this level (Figs. 5C, 7 and 8A). In SEM images the stromatolites and hematite pigmentation show more or less regular network to flocculent ultrastructure or a honeycomb-like pattern of walls surrounding circular pits (Fig. 8B, C). Electron microprobe analyses demonstrate that the iron phase of the ooids and stromatolites is represented by iron-rich chlorite

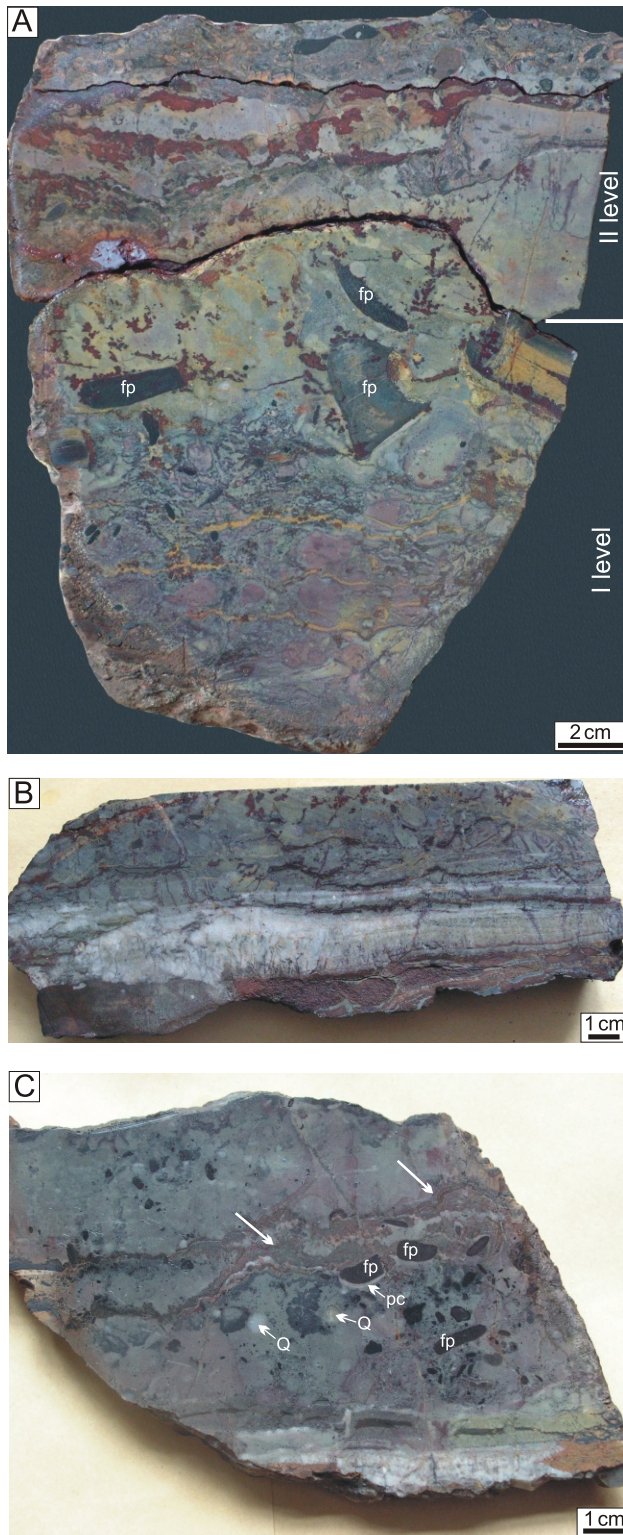


Fig. 5. Polished slab of the composite limestone bed with red hematite pigmentation (blisters, perforation and microfissure infillings)

A — brecciated limestone of level I revealing diagenetic colour mottling and dark phosphorite pebbles (fp) overlain by reworked limestone of level II; **B** — thin calcite layer at the base of the composite limestone bed; **C** — thin calcite layer overlain by limestone with dark phosphorite pebbles (fp), quartz grains (Q) and dark grains floating within carbonate background; note tiny Fe microstromatolites showing crude lamination (white arrows) and pendant calcite cement underneath dark phosphorite pebbles (pc)

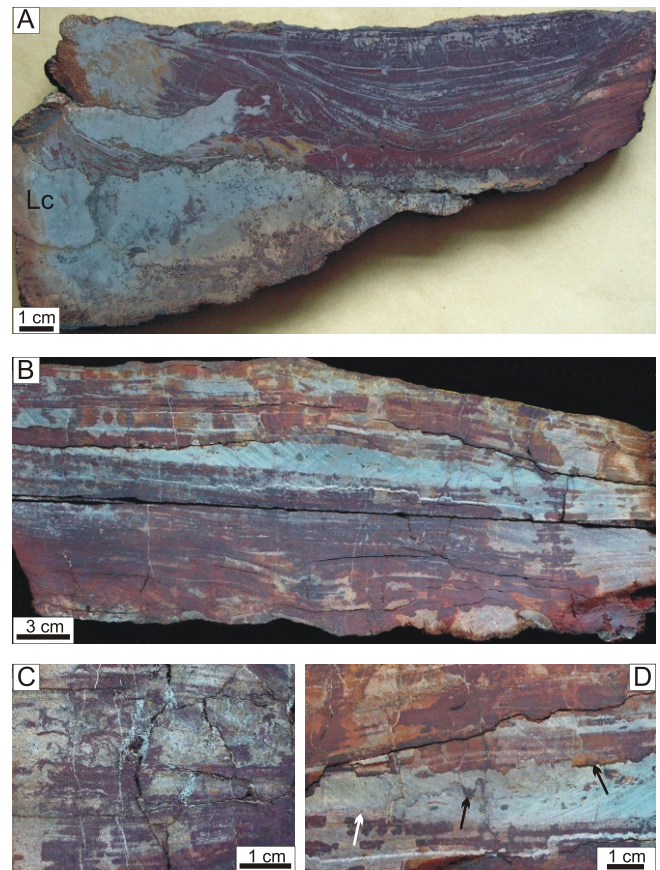


Fig. 6. Polished slab of the laminated red bed

A — continuous transition from the composite limestone bed (level II) with scattered iron ooids to laminated red limestone, Lc — limestone clast; **B** — thin pale grey limestone interbedded occurring within the middle portion of the red laminated limestone; **C** — tiny columns and sediment mottling referable to microbial origin visible within the red laminated limestone; **D** — tiny columns (white arrow) occupying the base of the limestone layer (shown in B); note a sutured small-scale discontinuity surface covered by an Fe impregnated crust at the top of this layer (black arrows)

(Fig. 8A, D) referred herein to “chamositic clay mineral” (Van Houten and Purucker, 1984). These authors introduced this as a general term for iron-rich A trioctahedral serpentinite (berthierine) and iron-rich 1A trioctahedral (chlorite). In addition, the iron-rich chlorite phase is ubiquitously associated with interparticle porosity of the host limestone. However, in the case of the black coated grains the dominant iron phase is opaque ferric oxides (goethite) replacing the primary chamositic mineral. The black grains are oval to irregularly shaped and contain inclusions of detrital terrigenous silt, and in some cases, they display poorly defined thin cortical laminae (Figs. 7 and 9A, B, C). Thus, their structure is consistent with iron pisoids/ooids or even with spheroidal spongiostromate/porostromate oncoids; however, some of these grains seem to be fragments of iron-rich sediment. In addition, they reveal circumgranular cracking filled with fine-grained sediment or calcite cement, whereas some parts of these grains are completely leached and replaced by fibrous or blocky calcite cement (Fig. 9A, B, C).

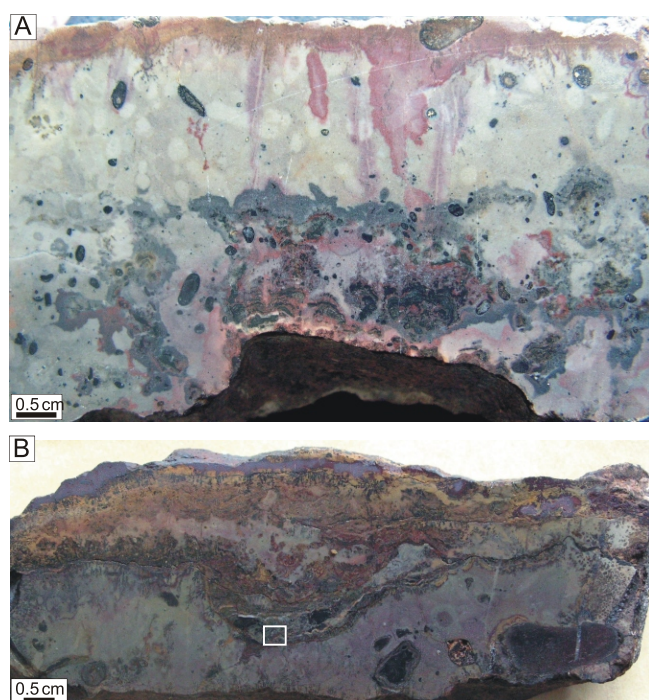


Fig. 7. Polished slab showing Fe microstromatolites occurring upon the discontinuity surfaces — hardground

Note black iron-rich grains within the host limestone and laminar coating on large grains (B — bottom right); the box marks a photomicrograph of the microstromatolite visible in Figure 8D

Microscopically, the limestone of the level considered reveals fine to coarse crystalline microfabric with common crystal size mottling and displacive growth features (Figs. 9 and 10A). The fine crystalline sediment displays a mosaic of microspar to fine spar crystals with sparsely distributed coarser pseudospar (anhedral) crystals. The crystals show irregular intercrystalline boundaries; however, embayed large grains and floating-grain textures as well as leached skeletal grains occur in this dense crystalline groundmass. In some cases, the intercrystalline space is filled with the carbonate mud or iron-rich matrix. Under CL, this kind of microfabric displays nonluminescent crystals rimmed by brightly orange luminescent thin laminae; however, dull luminescent crystals occur also. The coarse crystalline fabric is represented by the inclusion-rich coarse blocky calcite cement accompanied by columnar crystals, which form a more or less irregular network in the finely crystalline or iron-rich background (Fig. 9D, E). Moreover, the blocky cement commonly fills the leached grains and rarely may be present as crystal silt within leached voids. Under CL, the coarse blocky crystals are usually nonluminescent but some of them reveal also nonluminescent to bright/dull zonation and irregular crystal boundaries (Fig. 10A, B). Electron microprobe analyses demonstrate an admixture of FeO (up to 2.20 wt.%) and MnO (up to 1.33 wt.%) within the blocky calcite crystals. The outer surfaces of large voids, fractures or fragments of host sediment are commonly rimmed by dendritic and radial fibrous high Mg calcite cement (Fig. 10A, C, D). The latter one consists of cloudy or turbid, fibrous to bladed crystals (up to several millimetres long) growing perpendicu-

larly to the substrate and exhibiting straight to undulose extinction (Fig. 10C, D). The dendritic calcite together with blocky calcite commonly fills the large voids or interporosity space. The elongated columnar radial fibrous calcite forming isopachous crusts are the dominant cement morphology within calcite layers and lenses occurring in the lower portion of the level considered (Fig. 5B, C). These crystals reach several millimetres in length and reveal many inclusions and a low iron content. In CL they are predominantly nonluminescent with only thin brightly luminescent envelopes in the outer parts of the crystals (Fig. 10E). The other kind of calcite cement includes clear bladed or blocky crystals occurring as patchy concentrations, an irregular network, or as a circumgranular cement surrounding some grains and pebbles (Fig. 9D, E). In places, they form a pendant or microstalactitic cement underneath the pebbles or below the discontinuity surfaces (Fig. 9B, C). Locally, the clear blocky cement fills the complex irregular cracks, which form irregular networks or patchy concentrations emplaced upon the microfabrics characterized above.

Level II — reveals a relatively high rate of sediment reworking indicated by the presence of limestone clasts showing petrographic features consistent with carbonate sediment from the underlying level (Fig. 11A). A common feature of this level are tiny Fe-stromatolite-like structures composed of the chamositic phase and replaced locally by hematite, and resting on small-scale indurated discontinuities (Fig. 11A). In some cases, these structures encrust the limestone clasts but in places they are reworked and replaced upwards by iron pisoids and ooids (Fig. 11). Electron microprobe analyses demonstrate that these coated grains are composed of iron-rich chlorite referable to chamosite or berthierine. The brown/green pisoids (up to 1.5 cm in diameter) display an ellipsoidal shape with fine concentric cortical laminae. They are mixed with worn skeletal grains and iron ooids, and are concentrated largely at a minor discontinuity surface. The iron ooids in this horizon are commonly crushed and distorted, and show a laminar fabric (Fig. 11B). However, upwards they are represented by well-preserved yellow to brown superficial ooids (up to 1.0 mm in diameter) with a poorly laminated cortex, scattered within the carbonate background (Figs. 6A and 12A). Their nucleus displays an iron-rich irregular internal structure with a small admixture of detrital terrigenous silt, and circumgranular and septarian micro-cracking filled by the light calcite cement (Fig. 12A, B). The chamositic phase in pisoids and ooids is replaced by kaolinite and blocky or fibrous calcite obliterating their primary structure (Figs. 11C and 12B, C, D, E).

Laterally, the second level may be represented by a conglomerate bed, up to 10 cm thick, consisting of limestone and iron-rich clasts of various sizes, mixed with iron pisoids and pisoids/ooids (Fig. 13A). The iron-rich clasts are represented by massive chamosite and hematite as well as by Fe-stromatolite mats. The latter clasts are commonly distorted and consist of alternating laminae composed of opaque iron oxides (goethite/hematite) and chamosite replaced locally by clear blocky calcite cement (Fig. 13B). In turn, the limestone clasts are much better rounded and display a cement morphology consistent with limestone of the first level, including dendritic and radial fibrous calcite (Fig. 13A). Some clasts are

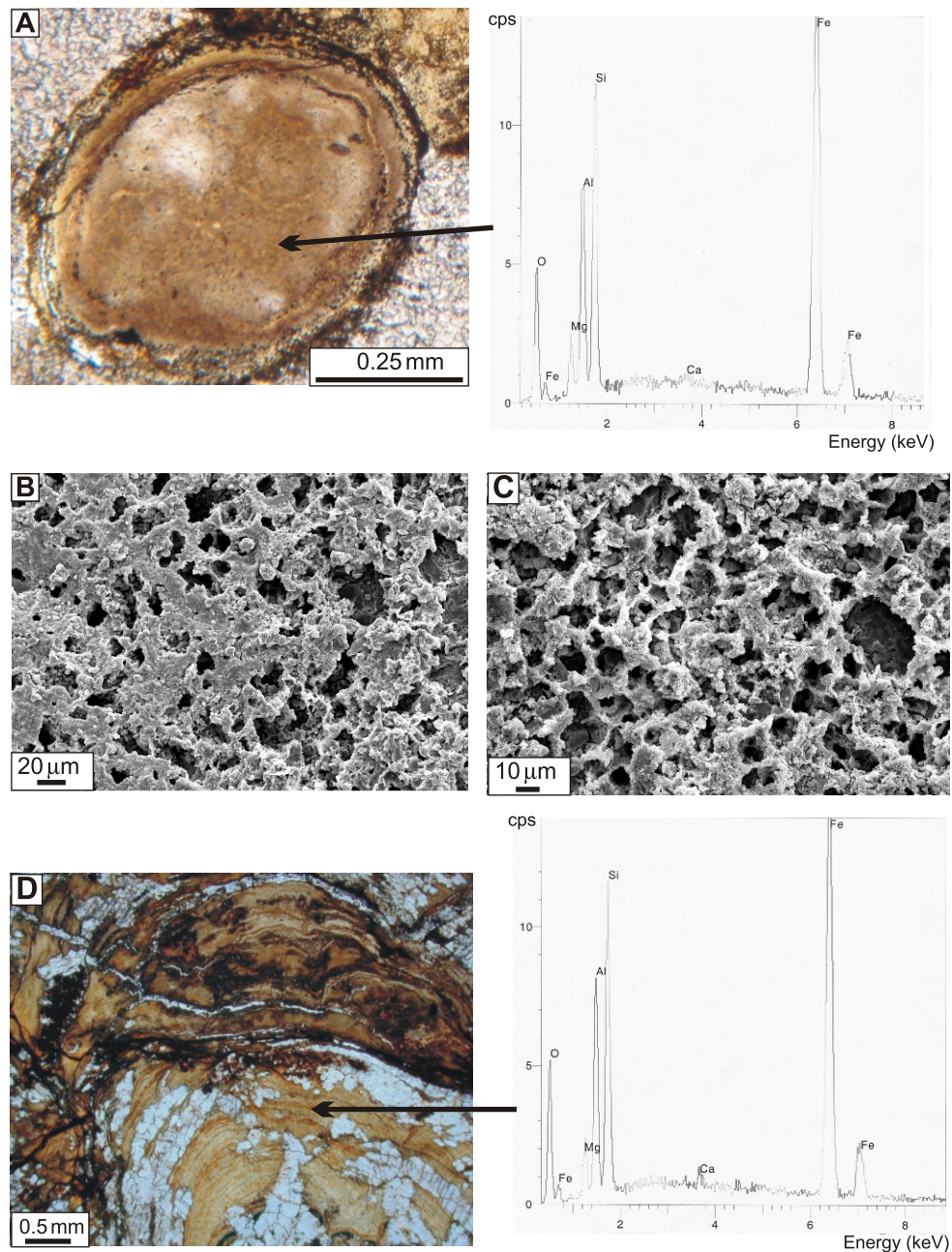


Fig. 8A — photomicrograph of a superficial iron ooid and its chemical composition, plane-polarized light (PPL); **B, C** — SEM images of the hematite pigmentation showing a more or less regular network to a flocculent ultrastructure (**B**) and tiny Fe-stromatolites revealing a honeycomb-like pattern of walls surrounding circular pits (**C**); **D** — photomicrograph of Fe-stromatolites (shown in **Fig. 7B**) and its chemical composition; note calcite replacements within this structure, PPL

composed of iron-rich micrite-sized carbonate with an admixture of silt- to sand-size quartz grains and circumgranular cracking (**Fig. 13C**).

LAMINATED RED BED (LR)

The base of this bed is delineated by a Fe-stained discontinuity; however, in some places there is continuous sedimentary transition from the underlying iron ooid-bearing limestone (**Fig. 6A**). The bed shows distinct lamination expressed by red

and pale grey laminae (**Fig. 6A, B**). The light laminae consist of coarse calcite crystals, whereas the red laminae are composed of opaque iron oxides that show a blister to tuft-like pattern mixed with calcite crystals. Locally, tiny microbial columns and sediment mottling can be visible in some parts of this bed (**Fig. 6C**). In places, the calcite laminae observed microscopically reveal recrystallized globular structures or microcolumns resembling the organic microfabric. A thin (up to 1.5 cm) pale grey limestone layer with scattered crinoids and brachiopods occurs within the middle portion of this bed (**Fig. 6B**). The base of this

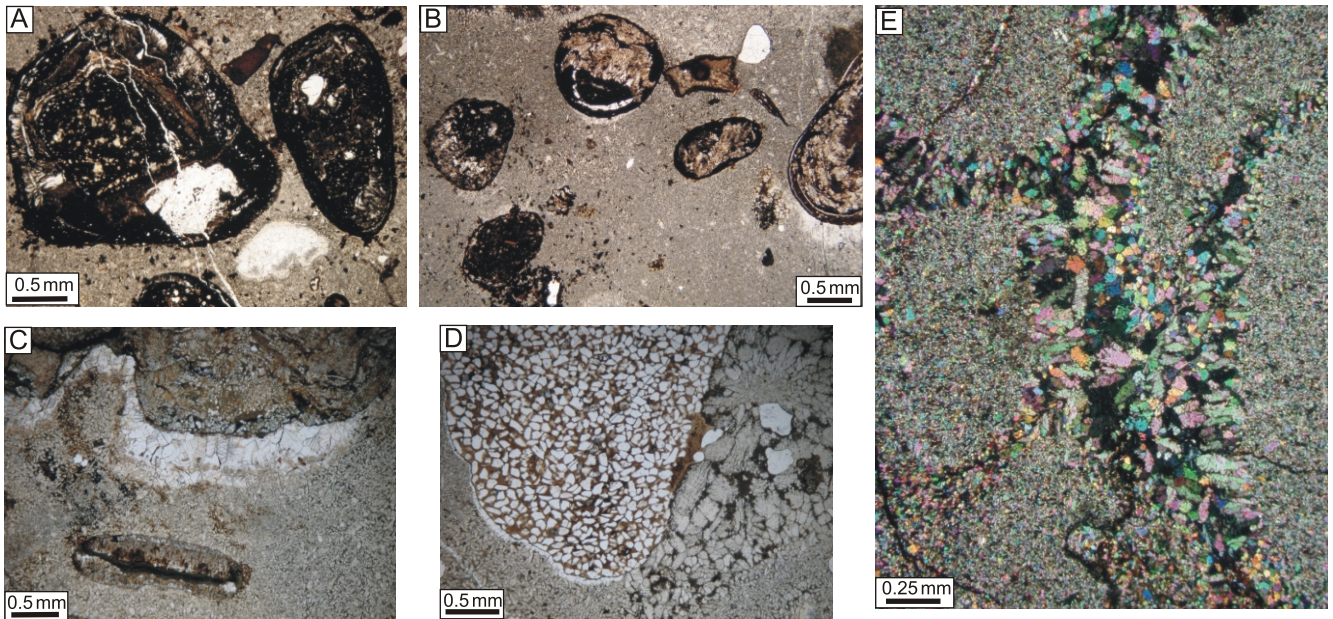


Fig. 9A–B — photomicrograph showing black iron ooids revealing inclusions of detrital terrigenous silt, calcite replacement and circumgranular cracking; the grains float within a fine crystalline microfabric; note the pendant cement on the lower surfaces of ooids (B), PPL; **C** — photomicrograph of microstalactitic cement underneath a small discontinuity surface; the host limestone shows a fine crystalline microfabric; note black iron ooid with fibrous calcite replacement in the lower part of the picture, PPL; **D** — photomicrograph indicating coarse crystalline fabric represented by the inclusion-rich coarse blocky calcite cement accompanied by tiny columnar crystals replacing the fine crystalline microfabric, note circumgranular cement on the lower surface of the phosphorite pebble, PPL; **E** — photomicrograph showing coarse crystalline fabric forming a more or less regular network within the finely crystalline background, crossed polars (XPL)

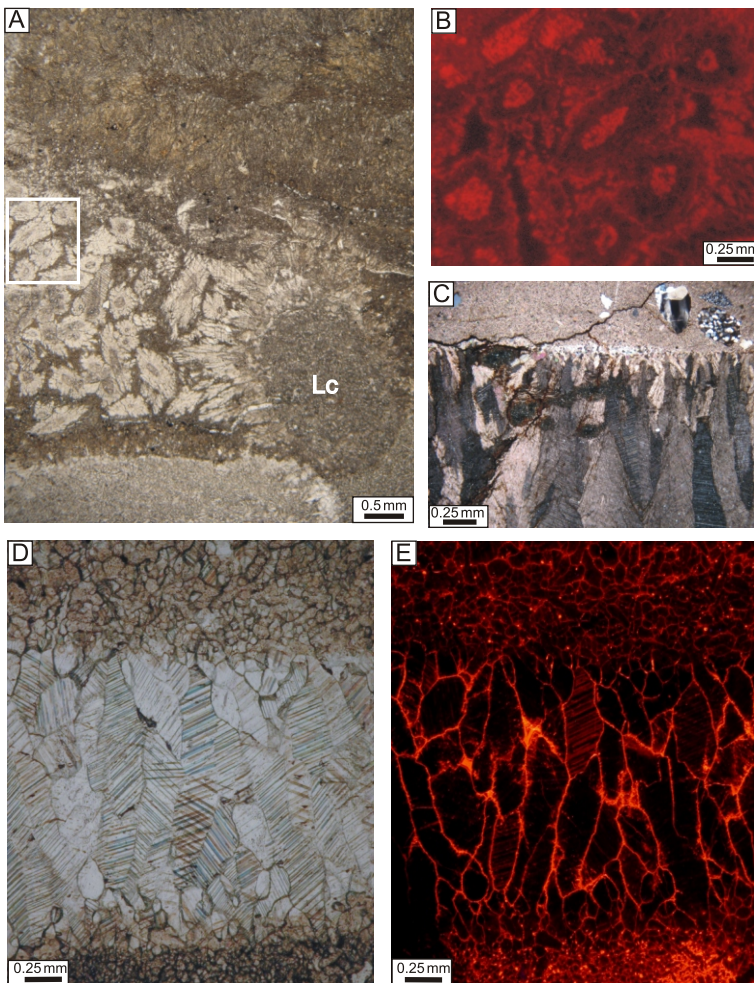


Fig. 10A — photomicrograph showing dense micrite to microsparite groundmass (upper portion) within portion of coarse crystalline fabric (left part), note rim of dendritic and radial fibrous calcite on clast (Lc) derived from the background carbonate, PPL; **B** — CL image of coarse crystalline calcite (marked on A) showing nonluminescent to bright/dull zonation and irregular crystal boundaries; **C–E** — photomicrographs of elongated columnar radial fibrous calcite forming isopachous crusts that are the dominant cement morphology within calcite layers (shown in Fig. 5B, C), XPL (C), PPL (D); under CL (E) these crystals are nonluminescent with only thin brightly luminescent outer envelope

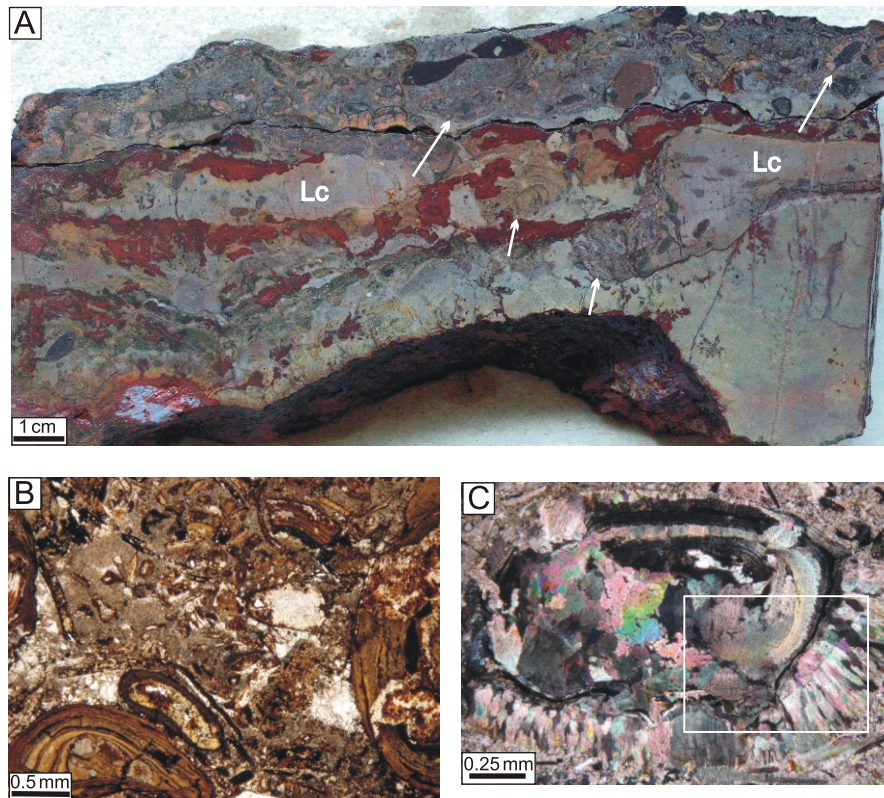


Fig. 11A — polished slab of reworked limestone of level II with limestone clasts (Lc) showing petrographic features consistent with carbonate sediment of the underlying level; tiny Fe-stromatolite-like structures occur on the small-scale discontinuities or encrust the limestone clasts (short arrows), they are commonly replaced by hematite; the iron pisoids with calcite replacement occur in the uppermost part of the bed (long arrows); **B** — photomicrograph of crushed iron ooids (chamositic) accompanying the pisoids, PPL; **C** — photomicrograph of iron pisoid replaced by blocky and acicular calcite cements (from the upper part of the bed visible on A), XPL

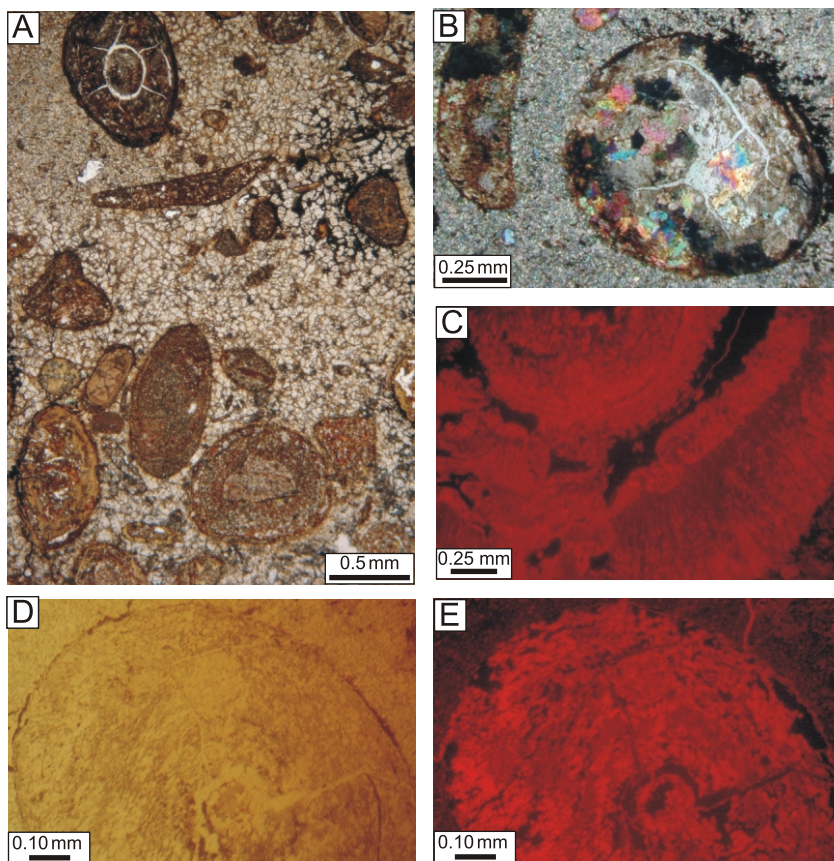


Fig. 12A — photomicrograph showing iron ooids floating within fine crystalline background; note fine cortical lamination of ooids and septarian micro-cracking, PPL; **B** — photomicrograph of iron ooid replaced by blocky calcite cement, note septarian micro-cracks inside the grain, XPL; **C** — CL photomicrograph of fibrous calcite cement replacing iron pisoid (marked in Fig. 11C) displaying dull luminescence; **D, E** — photomicrograph of iron ooid with fine shrinkage cracks, completely replaced by calcite cement, **D** — PPL, **E** — CL

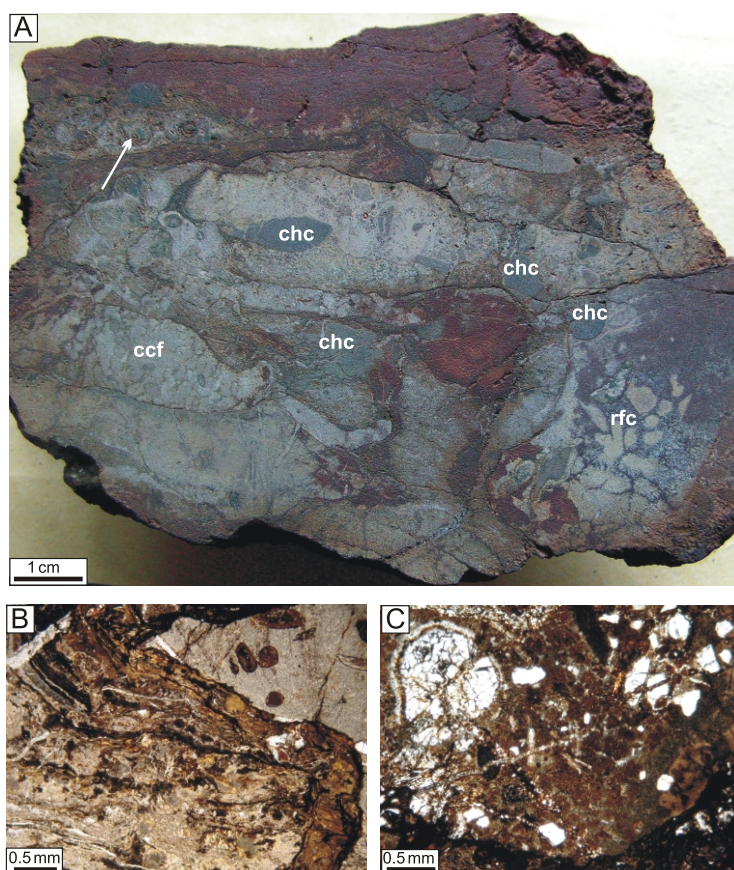


Fig. 13A — polished slab of conglomerate bed composed of limestone and iron-rich clasts — regolith, the cement morphology within the limestone clasts includes fine to coarse crystalline fabric (ccf) and radial fibrous calcite (rfc), note chamosite clasts (chc) within the conglomerate and iron pisoids above it (long arrow); **B** — photomicrograph showing Fe stromatolite clast with calcite replacement, PPL; **C** — photomicrograph of iron-rich micrite-sized carbonate clast showing admixture of silt- to sand-size quartz grains and circumgranular cracking, PPL

layer is occupied by sparsely-spaced tiny microbial columns, whereas the top is delineated by a sutured small-scale discontinuity surface covered by the Fe-impregnated crust (Fig. 6D)

DISCUSSION

SEDIMENTARY ENVIRONMENT

The conspicuous discontinuity at the base of the Pobroszyn Formation, reported both from the type section and from borehole logs, marks a major change in the depositional conditions of the primary sediments. The stratification pattern of the composite limestone bed allows two stages in its development to be distinguished. The first stage was coeval with the deposition of level I, which reveals features commonly noted in condensed sections and hardgrounds of pelagic realms. The sedimentary conditions of this level were dominated by non-deposition periods or by a low sedimentation rate favouring precipitation of an authigenic Fe phase, which impregnated the minor discontinuities and pore spaces and also allowed microstromatolites to thrive close to the sediment-water interface. Level I was deposited in an open marine setting isolated from the source of

terrigenous material; however, some pebbles, quartz grains and black coated grains were occasionally delivered there. It is noteworthy that starved open marine conditions of the Palaeozoic are postulated for *in situ* development of iron ooids (Young, 1989, 1992), which accompany the minor discontinuities occurring within this level. The black grains, showing microfabric consistent with soil pisoids/ooids or fragments of iron-rich soils (see Siehl and Thein, 1989), might have been derived by storms from areas undergoing weathering that were located close to the marginal marine zone. The relationship of chamosite with microstromatolite structures suggest that microbial activity may have contributed to precipitation of the iron phase. The honeycomb-like pattern of these structures in SEM images may correspond to organic material (exopolymeric substances) of bacterial origin that was capable of engulfing a variety of metals, e.g. iron (McLean *et al.*, 1996; Pr eat *et al.*, 1999). Taylor and Curtis (1995) indicate that berthierine, which is interpreted as the precursor of chamosite, precipitates during the early period of suboxic diagenesis when sulphide activity in pore water is low. In the case studied these conditions might have been achieved through fluctuations of the redox boundary below the microbial community.

The second phase in development of the composite bed (level II) was closely controlled by intense reworking, which resulted in the concentration of limestone, hematite and Fe-stromatolite clasts in the conglomerate bed. However, the high energy events were interrupted by periods of non-deposition that favoured colonisation of the substrate by microbial communities contributing to Fe authigenesis. Their erosion and then deposition together with limestone and hematite clasts indicate that the sedimentary regime of level II has experienced multiple phases of reworking and Fe authigenesis. The abundance of iron-coated grains in the uppermost portion of this level mixed with some limestone clasts and worn skeletal fragments indicate that the iron pisoids and ooids were also re-deposited. Thus, the sedimentary record of the level II fits precisely to a two-stage depositional history of iron ooids, which were winnowed and reworked from the source area to be finally accumulated together with skeletal material at the site of deposition. It is consistent with the widely accepted idea that reworking and winnowing processes are important agents driving replacement of iron ooids and pisoids from terrestrial and marginal marine settings or offshore swells into the open marine environment (Siehl and Thein, 1989; Young, 1989, 1992; Cotter, 1992).

DIAGENETIC ENVIRONMENT

Level I of the composite limestone bed reveals microscopic features suggesting early diagenetic alteration of the parent carbonate sediment. The rims of bladed and blocky circumgranular calcite cement on some grains and clasts as well as the radiaxial fibrous crystals on the surfaces of pores and cavities are diagnostic of a shallow marine setting, e.g., beach shoreface (Inden and Moore, 1983; James and Choquette, 1990a; Moore, 2001). This kind of cementation is common in the marine phreatic zone (Tucker and Wright, 1990; James and Choquette, 1990b; Moore, 2001), but rare examples of pendant and microstalactitic cements within the limestone studied suggest also marine vadose conditions. The calcite layers and lenses at the base of the composite bed show features of fibrous radiaxial crusts, which are characteristic of marine and meteoric environments. Their microfabric is somewhat similar to speleothems considered as precipitates indicative of emergence and karstification (Thraillkill, 1976; Folk and Assereto, 1978; Esteban and Klappa, 1983; Vera *et al.*, 1988). In freshwater environments, the radiaxial palisade fabric is interpreted as recrystallized stromatolites that underwent multiple neomorphic changes (Freytet and Verrecchia, 1998, 1999). The occurrence of variably sized and oriented calcite-filled cracks indicates that desiccation and expansive growth followed by calcite precipitation were important agents controlling the microfabric pattern of the composite limestone bed.

A number of macroscopic features suggest meteoric overprint upon the parent limestone. They include diagenetic colour mottling, incipiently brecciated sediment and Fe-staining. In addition, the microfabric of this level indicates replacive and destructive calcite growth (e.g. a floating grain texture and rare embayed grains) that may be referred to fine crystal-sized alpha calcite (*sensu* Tucker and Wright, 1990; Wright, 1994; Wright and Tucker, 1991). Further evidence for meteoric

diagenesis comes from the complex irregular cracks or tiny fractures filled by more coarsely crystalline calcite within the finely crystalline background, which appear to reflect the conduits of meteoric waters. Other early diagenetic features typical of the meteoric diagenetic environment include blocky calcite cement replacing the iron ooids as well as circumgranular and septarian cracking within these grains.

CL observations provide additional support for the meteoric origin of the microfabric of the composite limestone bed. The CL pattern of the fine crystalline groundmass as well as the radiaxial fibrous and blocky cements indicates a predominance of nonluminescent calcite, reflecting the apparently oxidized nature of the shallow meteoric waters (Meyers, 1974, 1978; Grover and Read, 1983; Choquette and James, 1988; Neimann and Read, 1988, Wright and Peeters, 1988; Tucker and Wright, 1990). Thin brightly luminescent outer laminae and zones suggest an influence of reducing conditions (Meyers, 1991; Tucker and Wright, 1990). The occurrence of both luminescent (bright to dull) and nonluminescent calcite zones within some coarse calcite crystals appears to reflect changes of redox conditions possibly brought about in the shallow phreatic zone as a result of fluctuations in the level of the water table. This is supported by irregular crystal outlines produced by precipitation and dissolution of crystals during fluctuating levels of CaCO₃ saturation.

SEDIMENTATION AND DIAGENESIS IN THE CONTEXT OF SEA LEVEL CHANGES

The biostratigraphic and sedimentary data indicate that the discontinuity at the base of the Pobroszyn Formation includes a hiatus corresponding to the Floian stage and locally to the upper Tremadocian. A comparable break of sedimentation, initiated in the late Tremadocian and lasting up to the late Darriwilian, has been documented in some localities of the southern HCM (Trela, 2006b). By contrast, a significant sea level rise, interrupted by a few third order sea level falls, has been documented on Baltoscandia during the Floian stage (Nielsen, 2004). Thus, data from the HCM indicate that regional tectonic activity might have been an important agent responsible for development of the unconformity (regional sequence boundary) at the base of the Pobroszyn Formation. As can be inferred from the biostratigraphic record (Dzik, 1999), the deposition of the Pobroszyn Formation was coeval with the early Middle Ordovician sea level rise (*navis* Zone) correlated with the Gärdlosa drowning on Baltoscandia (Nielsen, 2004). In the southern HCM, the same transgression was responsible for deposition of the Szumsko Formation (Trela, 2006a, b; Fig. 4).

The sedimentary and diagenetic history of the Pobroszyn Formation might have been closely associated with a palaeohigh postulated by Kowalczewski (1994) in the central HCM (Fig. 4). The local tectonic activity (faulting) affecting this palaeohigh along with a drop in sea level might have resulted in location of the Pobroszyn Formation within the marginal shoreface setting and with early diagenetic cementation within a marine phreatic environment. However, some sedimentary and petrographic features suggest partial emergence of the Pobroszyn locality and subsequent meteoric diagenesis of the primary limestone. With changes of sea level, complex patterns of superimposed coastal and subaerial processes may act

on the same exposed surface. Reworking of the lithified carbonate substrate within the coastal zone was an important agent controlling the sedimentary record. Data derived from the Jeleniów 2 borehole indicate the multiple destruction of the lithified substrate.

Stratigraphic data allow correlation of this early diagenetic cementation and meteoric overprint in the Pobroszyn Formation with the early and middle Darriwilian sea level (late Arenig–early Llanvirn) lowstand interval in Baltoscandia (Nielsen, 2004). In the southern HCM, the same lowstand interval is recorded by sandstones of the Bukówka Formation (Fig. 4), deposited in a shallow nearshore environment (Trela, 2006b).

The level II of the composite bed appears to represent a new sedimentary phase associated with the following transgression, which probably reworked the underlying indurated substrate or regolith horizon (conglomerate bed) associated with preceding lowstand interval. Marine flooding was also responsible for re-deposition of iron pisoids and ooids (commonly deformed and crushed) from marginal or terrestrial settings. Some carbonate clasts, with terrigenous clastic detritus and circumgranular cracking, appear to be derived from reworked carbonate microcrystalline soil crusts. The overlying red laminated limestone bed can be interpreted as an iron-stromatolite deposited during the maximum flooding stage or even the early phase of sea level highstand. Its sedimentary record suggests that this bed experienced a reduced sedimentation rate (or even omission conditions) coupled with formation of the Fe crust. The leaching and circumgranular/septarian cracking of iron pisoids and ooids and their replacement by clear blocky and fibrous calcite cements suggest that the sedimentary record of the second level, as with the underlying limestone, was altered to some extent by meteoric processes. This can be also inferred from the occurrence of kaolinite replacing the chamosite phase within the leached iron coated grains. This kind of replacement in ironstones is postulated to be product of early diagenesis or subaerial weathering (Kearsley, 1989). In addition, meteoric waters likely contributed to the replacement of chamosite by ferric oxides (see Mücke and Doering, 1994), which form the dominant Fe phase within the tiny stromatolites of level II and

the red laminated bed. However, it seems plausible that hematite replacement originated from autooxidation of Fe^{2+} by a mat-forming bacterial community growing under microaerophilic conditions in open and calm marine waters (see Pr at *et al.*, 1999).

CONCLUSIONS

Middle Ordovician deposits in the northern Holy Cross Mts. (Łysog ry Unit of central Poland) were temporarily exposed in a trench dug in Pobroszyn. They are represented by two beds, 25 and 15 cm thick respectively, which form a condensed unit dated by means of conodonts of the *navis* Zone. The basal limestone bed reveals a complex stratification pattern reflecting alternating sedimentary conditions. The occurrence of a conodont fauna indicates that this limestone was deposited in the open marine realm during the early Middle Ordovician sea level rise (*navis* Zone) coeval with the G rdlosa drowning on Baltoscandia. A relatively low sedimentation rate of this bed favoured early diagenetic Fe authigenesis mediated by benthic microorganisms. It is noteworthy that this limestone displays features suggesting early diagenetic alteration of the parent carbonate sediment in a marginal marine setting (e.g., shoreface) or even meteoric environment produced during subsequent sea level fall. The higher reworked part of the lower bed appears to represent a renewed depositional phase associated with a second transgressive event. High energy events were interrupted by non-deposition periods favouring development of benthic microbial communities contributing to Fe authigenesis. The overlying red laminated limestone bed can be interpreted as an iron-stromatolite deposited during the final stage of the second transgression or even during the early phase of sea level highstand.

Acknowledgments. This paper is a contribution to IGCP 503 project “Ordovician Palaeogeography and Palaeoclimate”. I am grateful to dr hab. J. Szulc and dr J. Wheeley for reading the first version of manuscript and for helpful comments.

REFERENCES

- COCKS R. M. and TORSVIK T. H. (2005) — Baltica from the late Precambrian to mid-Palaeozoic times: the gain and loss of a terrane's identity. *Earth-Sc. Rev.*, **27**: 39–66.
- COTTER E. (1992) — Diagenetic alteration of chamositic clay minerals to ferric oxide in oolite ironstone. *J. Sediment. Res.*, **62**: 54–60.
- CHOQUETTE P. W. and JAMES N. P. (1988) — Introduction. In: *Paleokarst* (eds. N. P. James and P. W. Choquette): 1–21. Springer-Verlag, New York.
- DADLEZ R., KOWALCZEWSKI Z. and ZNOSKO J. (1994) — Niekt re kluczowe problemy przedpermskiej tektoniki Polski. *Kwart. Geol.*, **38** (2): 169–190.
- DZIK J. (1999) — The Ordovician in the Holy Cross Mountains. In: *International Symposium on the Ordovician System, ISOS Prague 1999, Pre-Conference Field trip, Excursion guide Poland and Germany* (eds. J. Dzik, U. Linnemann and T. Heuse): 3–7.
- ESTEBAN M. and KLAPPA C. F. (1983) — Subaerial exposure environment. In: *Carbonate Depositional Environments* (eds. P. A. Scholle, D. G. Bebout, C. H. Moore). AAPG, Memoir, **33**: 1–54.
- FOLK R. L. and ASSERETO R. (1978) — Comparative fabrics of length-slow and length-fast calcite and calcitized aragonite in a Holocene speleothem, Carlsbad caverns, New Mexico. *J. Sediment. Petrol.*, **46**: 486–496.
- FREYTET P. and VERRECCHIA E. P. (1998) — Freshwater organisms that build stromatolites: a synopsis of biocrystallization by prokaryotic and eukaryotic algae. *Sedimentology*, **45**: 535–563.
- FREYTET P. and VERRECCHIA E. P. (1999) — Calcitic radial palisadic fabric in freshwater stromatolites: diagenetic and recrystallized feature or physicochemical sinter crust? *Sediment. Geol.*, **126**: 97–102.

- GROVER G. A. and READ J. F. (1983) — Regional cathodoluminescent patterns, middle Ordovician ramp carbonates, Virginia. *Am. Ass. Petrol. Geol., Bull.*, **67**: 1275–1303.
- INDEN R. F. and MOORE C. H. (1983) — Beach Environment. In: *Carbonate Depositional Environments* (eds. P. A. Scholle, D. G. Bebout and C. H. Moore). AAPG, Memoir, **33**: 211–265.
- JAMES N. P. and CHOQUETTE P. W. (1990a) — Limestones — the sea-floor diagenetic environment. In: *Diagenesis* (eds. I. A. McIlreath and D. W. Morrow). Geosc. Canada, Reprint Ser., **4**: 13–34.
- JAMES N. P. and CHOQUETTE P. W. (1990b) — Limestones — the meteoric diagenetic environment. In: *Diagenesis* (eds. I. A. McIlreath and D. W. Morrow). Geosc. Canada, Reprint Ser., **4**: 35–73.
- KEARSLEY A. T. (1989) — Iron-rich ooids, their mineralogy and microfabric: clues to their origin and evolution. In: *Phanerozoic Ironstones* (eds. T. P. Young and W. E. G. Taylor). Geol. Soc., Spec. Publ., **46**: 141–163.
- KOWALCZEWSKI Z. (1994) — The Holy Cross Mts. in the Early Paleozoic. In: *Europrobe. Trans-European Suture Zone Workshop. Excursion Guidebook the Holy Cross Mountains, Kielce, 24 September – 1 October, 1994* (eds. Z. Kowalczewski, M. Szulczewski, Z. Migaszewski and K. Janecka-Styrz): 1–18.
- MCLEAN R. J. C., FORTIN D. and BROWN D. A. (1996) — Microbial metal-binding mechanisms and their relation to nuclear waste disposal. *Can. J. Microbiol.*, **42**: 392–400.
- MEYERS W. J. (1974) — Carbonate cement stratigraphy of the Lake Valley Formation (Mississippian) Sacramento Mountains, New Mexico. *J. Sediment. Petrol.*, **44**: 837–861.
- MEYERS W. J. (1978) — Carbonate cements — their regional distribution and interpretation in Mississippian limestones of southwestern New Mexico. *Sedimentology*, **25**: 371–400.
- MEYERS W. J. (1991) — Calcite cement stratigraphy: an overview. In: *Luminescence microscopy: quantitative and qualitative aspects* (C. E. Baker and O. C. Kopp., SEPM, Short Course, **25**: 133–147.
- MOORE C. H. (2001) — Carbonate reservoirs — porosity evolution and diagenesis in a sequence stratigraphic framework. *Develop. Sediment. Elsevier*.
- MÜCKE A. and DOERING Th. (1994) — Postdiagenetic ferruginization of Phanerozoic (oolitic) ironstones: a contribution to their genesis. In: *Development in Sedimentology*, **51**, *Diagenesis*, 4 (eds. K. H. Wolf and G. V. Chilingarian): 396–423.
- NAWROCKI J., DUNLAP J., PECSKAY Z., KRZEMIŃSKI L., ŻYLIŃSKA A., FANNING M., KOZŁOWSKI W., SALWA S., SZCZEPANIK Z. and TRELA W. (2007) — Late Neoproterozoic to Early Palaeozoic palaeogeography of the Holy Cross Mountains (Central Poland): an integrated approach. *J. Geol. Soc., London*, **164**: 405–423.
- NEIMANN J. C. and READ J. F. (1988) — Regional cementation from unconformity – recharged aquifer and burial fluids, Mississippian Newman Limestone, Kentucky. *J. Sediment. Petrol.*, **58**: 688–705.
- NIELSEN A. T. (2004) — Ordovician sea level changes: a Baltoscandian perspective. In: *The Great Ordovician Biodiversification Event* (eds. B. D. Webby, F. Paris, M. L. Drosser and I. G. Persival): 84–93. Columbia University Press, New York.
- PRÉAT A., MAMET B., BERNARD A. and GILLAN D. (1999) — Bacterial mediation, red matrices diagenesis, Devonian Montagne Noire (southern France). *Sediment. Geol.*, **126**: 223–242.
- READ J. F. and GROVER G. A. (1977) — Scalloped and planar erosion surfaces, Middle Ordovician limestones, Virginia: analogues of Holocene exposed karst or tidal rock platforms. *J. Sediment. Petrol.*, **47**: 956–972.
- SIEHL A. and THEIN J. (1989) — Minette-Type Ironstones. In: *Phanerozoic Ironstones* (eds. T. P. Young and W. E. G. Taylor). Geol. Soc., London, Spec. Publ., **46**: 175–193.
- TAYLOR K. G. and CURTIS C. D. (1995) — Stability and facies association of early diagenetic mineral assemblages: an example from a Jurassic ironstone-mudstone succession, U.K. *J. Sediment. Res.*, **A65**: 358–368.
- TOMCZYK H. and TURNAU-MORAWSKA M. (1967) — Zagadnienia stratygrafii i sedymentacji ordowiku Łysogór w nawiązaniu do niektórych profilów obszaru południowego. *Acta Geol. Pol.*, **17**: 1–46.
- THRAILKILL J. (1976) — Speleothems. In: *Stromatolites* (ed. M. R. Walter). *Developments in Sedimentology*, **20**: 73–86. Elsevier, Amsterdam.
- TRELA W. (2003) — Sedimentary environment of the Ordovician phosphate-bearing sequence in central Poland. In: *Proceedings of the 9th International Symposium on the Ordovician System* (eds. G. L. Albanesi, M. S. Beresi and S. H. Perlata). *INSUGEO Ser. Correl. Geol.*, **17**: 475–481.
- TRELA W. (2005) — Condensation and phosphatization of the Middle and Upper Ordovician limestones on the Malopolska Block (Poland): response to palaeoceanographic conditions. *Sediment. Geol.*, **178**: 219–236.
- TRELA W. (2006a) — Litostratygrafia ordowiku w Górach Świętokrzyskich. *Prz. Geol.*, **54** (7): 622–631.
- TRELA W. (2006b) — Ordowik w Górach Świętokrzyskich: zapis stratygraficzny i sedymentacyjny. In: *Procesy i Zdarzenia w Historii Geologicznej Gór Świętokrzyskich* (eds. S. Skompski and A. Żylińska): 28–35. LXXVII Zjazd Naukowy Polskiego Towarzystwa Geologicznego.
- TRELA W. (2008) — Sedimentary and microbial record of the Middle/Late Ordovician phosphogenetic episode in the northern Holy Cross Mountains, Poland. *Sediment. Geol.*, **203**: 131–142.
- TRELA W., SALWA S. and SZCZEPANIK Z. (2001) — The Ordovician rocks of Pobroszyn in Łysogóry region of the Holy Cross Mountains, Poland. *Geol. Quart.*, **45** (2): 143–154.
- TUCKER M. E. and WRIGHT V. P. (1990) — *Carbonate Sedimentology*. Blackwell.
- VAN HOUTEN F. B. (1985) — Oolitic ironstones and contrasting Ordovician and Jurassic palaeogeography. *Geology*, **13**: 722–724.
- VAN HOUTEN F. B. and PURUCKER M. E. (1984) — Glauconitic peloids and chamositic ooids — favourable factors, constraints, and problems. *Earth Sc. Rev.*, **20**: 211–243.
- VERA J. A., RUIZ-ORTIZ P. A., GARCIA-HERNANDEZ M. and MOLINA J. M. (1988) — Paleokarst and related pelagic sedimentation in the Jurassic of the Subbetic Zone, southern Spain. In: *Paleokarst* (eds. N. P. James and P. W. Choquette): 364–384. Springer-Verlag.
- WRIGHT V. P. (1994) — Palaeosols in shallow marine carbonate sequences. *Earth Sc. Rev.*, **35**: 367–395.
- WRIGHT V. P. and PEETERS C. (1988) — Origin of some early Carboniferous calcrete fabrics revealed by cathodoluminescence: implication for interpreting the site of calcrete formation. *Sediment. Geol.*, **65**: 345–353.
- WRIGHT V. P. and TUCKER M. E. (1991) — Calcretes: an introduction. In: *Calcretes* (eds. V. P. Wright and M. E. Tucker). *Internat. Ass. Sediment. Reprint Ser.*, **2**: 1–22.
- YOUNG T. P. (1989) — Phanerozoic ironstones: an introduction and review. In: *Phanerozoic Ironstones* (eds. T. P. Young and W. E. G. Taylor). Geol. Soc., Spec. Publ., **46**: ix–xxv.
- YOUNG T. P. (1992) — Ooidal ironstones from Ordovician Gondwana: a review. *Palaeogeogr., Palaeoclimat., Palaeoecol.*, **99**: 321–348.